Hindawi
Geofluids
Volume 2021, Article ID 6646311, 15 pages
https://doi.org/10.1155/2021/6646311

Research Article

Characteristics of Hydration Damage and Its Influence on Permeability of Lamellar Shale Oil Reservoirs in Ordos Basin

Pengfei Zhao,[1] **Xiangyu Fan**,[1,2] **Qiangui Zhang**,[1,2] **Bowei Yao**,[1] **Mingming Zhang**,[1] **Liang He**,[1] **Yu Qiang**,[1] **and Jinhua Liu**[1]

[1]*Southwest Petroleum University, Chengdu 610500, China*
[2]*National Key Laboratory of "Oil and Gas Reservoir Geology and Development Engineering", Southwest Petroleum University, Chengdu 610500, China*

Correspondence should be addressed to Pengfei Zhao; zpf2017@stu.swpu.edu.cn and Qiangui Zhang; qiangui.zhang@polymtl.ca

Received 22 December 2020; Revised 9 January 2021; Accepted 23 March 2021; Published 21 April 2021

Academic Editor: Keni Zhang

The continental shale oil reservoir has low permeability, high clay content, rich lamellar structure, and strong heterogeneity, which makes the reservoir vulnerable to hydration damage. In order to study characteristics of hydration damage and its influence on permeability of lamellar shale oil reservoirs, a series of experiments such as high-pressure mercury injection, steady gas permeability, rock thin section identification, and scanning electron microscope were carried out with the downhole core in Ordos Basin as the experimental object. The effects of water and water-based drilling fluid on pore size distribution, permeability, and rock microstructure were analyzed. Results show that the pore size of the reservoir is mainly nanoscale, and the pore size of shale changes most dramatically in the stage of hydration for 12-24 hours, while that of tuff changes most dramatically in 24-48 hours. The permeability increases rapidly with hydration time and then tends to be stable, among which the permeability of samples with lamellar structure in the direction parallel to the lamellar structure is most easily affected by hydration and changes fastest. Hydration leads to the formation of new pores, new fractures, and the expansion of existing fractures in rocks, especially in the strata containing large amounts of terrigenous clastic, lamellar structure, and pyrite. The new seepage channel increases the permeability of rock, and the soil powder and plugging particles in drilling fluid are easy to form protective mud cake in these places. These protective mud cakes not only change the microstructure of rock but also inhibit the influence of hydration on the pore space and permeability of rock, which play an effective role in preventing the mineral shedding on the rock surface, reducing the increase of micropores and delaying hydration.

1. Introduction

Shale oil is a kind of unconventional oil resources with great potential. It has large reserves and wide distribution in the world, which may become an important substitute for conventional oil in the future [1, 2]. The United States has changed from an oil-importing country to an oil-exporting country benefit from the successful commercial exploration and production of marine-sourced shale oil, which has aroused great attention to shale oil in the world [3, 4]. China is rich in shale oil reserves, and shale oil is mainly distributed in lacustrine basin. In recent years, the distribution characteristics, geochemical characteristics, and geological environment of shale oil reservoirs have been initially recognized through the exploration and research of Ordos Basin [5], Jianghan Basin [6], Bohai Bay Basin [7], Songliao Basin [8], and Jungar Basin [9]. However, due to the complex geological environment, strong heterogeneity, and high clay content of continental shale oil reservoir, drilling is difficult, which limits the efficient and safe development of shale oil in China [10].

Compared with oil-based drilling fluid, water-based drilling fluid (WBM) has lower cost and better environmental protection, and is widely used in drilling engineering [11]. There is high clay mineral content and complex pore structure in shale oil reservoir, which leads to hydration reaction when drilling with water-based drilling fluid [12]. The hydration reaction will lead to the increase of porosity, the

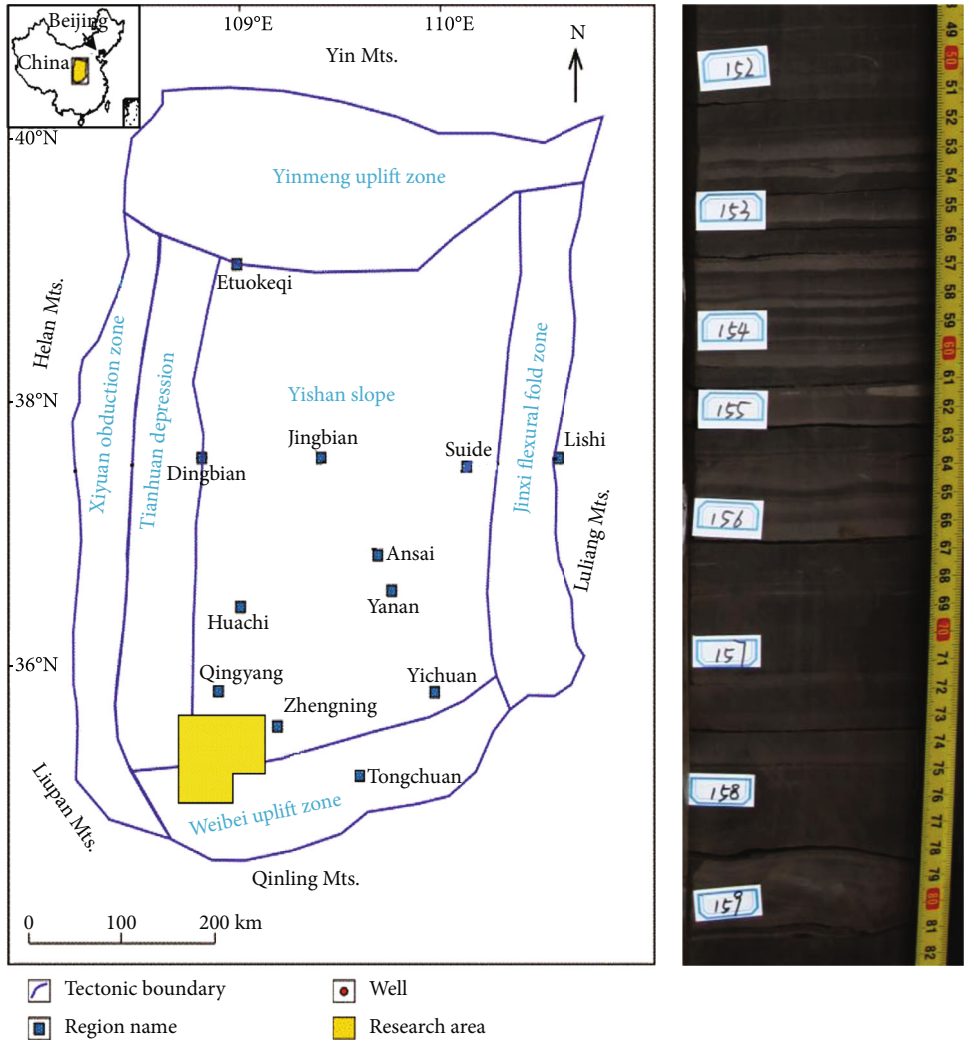

Figure 1: Continued.

(c)

Figure 1: (a) Geographical location characteristics of Ordos Basin and study area (modified after [33]). (b) Lamellar sandstone and bedding fractures in shale. (c) Bedding and structural fractures in tuff.

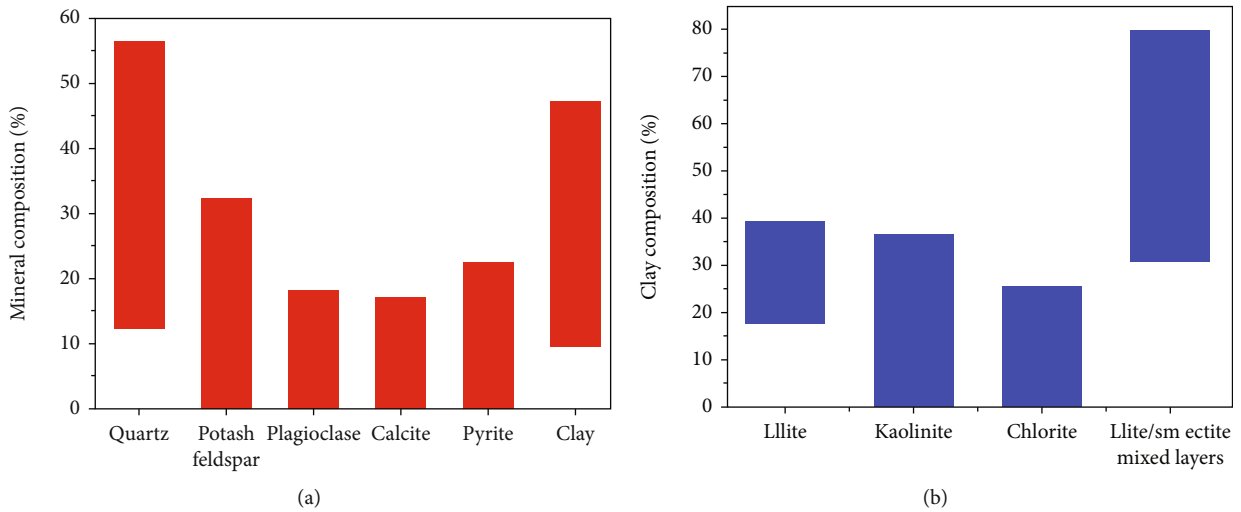

(a) (b)

Figure 2: Clay and mineral composition in work area (modified after [34]). (a) Content fluctuation range of different minerals. (b) Content fluctuation range of different clay.

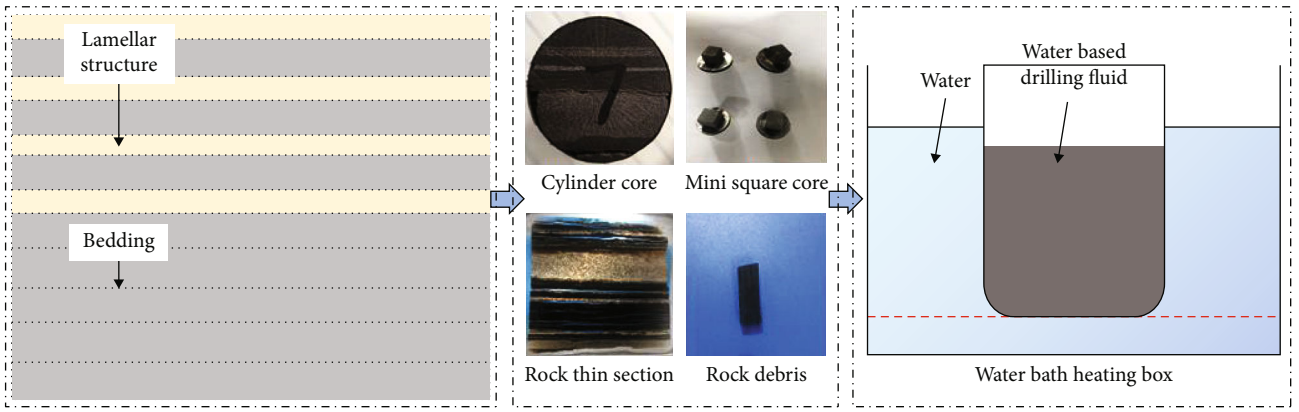

Figure 3: Samples preparation and hydration process.

looseness of internal structure, and the decrease of rock strength. Shale has obvious bedding structure, and microcracks are usually developed along the bedding, which provides a good channel for hydration [13]. The expansion stress produced by hydration will concentrate on the crack tip, which will cause fracture expansion and deformation and cause damage to the rock interior, such as borehole instability [14].

Through the experimental study of shale outcrop and core samples of Longmaxi formation in southern Sichuan Basin, Liu et al. analyzed the variation law of shale expansion stress under the influence of oil and water, and concluded that water-based drilling fluid is easy to cause wellbore instability [15]. Shi et al. used X-ray CT technology to observe the microstructure changes and crack propagation during the hydration process of hard brittle shale and concluded that secondary fracture failure caused by self-absorption is one of the main reasons for wellbore instability in hard brittle shale formation [16]. Ma and Chen carried out CT scanning on outcrop shale under different soaking time, and established a qualitative description method of shale hydration damage based on microstructure change [17]. Wang et al. carried out nuclear magnetic resonance (NMR) test on shale samples from Xi Feng formation after hydration damage and established a method to quantitatively explain shale hydration damage based on nuclear magnetic resonance [18]. Hydration damage not only changes rock structure and strength but also affects the permeability. Permeability reflects the migration ability of reservoir, which is one of the important parameters to evaluate reservoir. The permeability of unconventional reservoirs is very low, and the permeability of shale oil reservoirs is generally a few millidarcy [19]. Shale is dense, and its permeability is mainly provided by internal microfractures. Due to the bedding structure of shale, fractures are easy to distribute along the bedding, resulting in obvious anisotropy of shale permeability. N. R. Backeberg et al. studied the anisotropic permeability of shale by the nano-CT and found that the anisotropic permeability of shale is related to the anisotropy of initial fracture [20]. Ma et al. studied the permeability of Longmaxi shale and concluded that the permeability is related to the gas tested. Under the methane and nitrogen test, the permeability

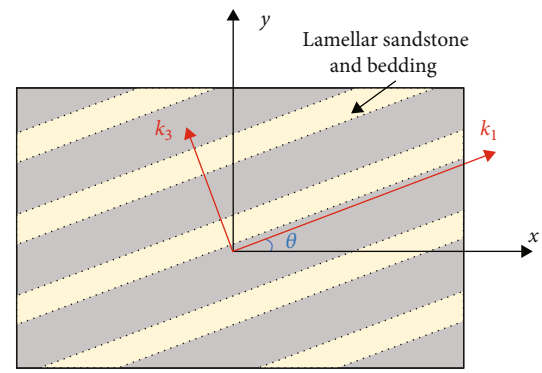

Figure 4: Relationship between permeability direction and lamellar structure in shale oil reservoir.

anisotropy ratio ranges from 5.2 to 510.5 [21]. They studied the influence of temperature and bedding direction on shale permeability by using high temperature triaxial steady-state permeability test system and obtained shale permeability anisotropy and its reasons under different temperatures and bedding directions [22]. It is more and more important for oil exploration and development to study the permeability variation characteristics of unconventional reservoirs under the influence of multiple factors.

As for the hydration damage of shale oil reservoir and its influence on permeability, the following contents need to be supplemented. First of all, the existing research object of hydration damage is usually the outcrop core of marine strata [23, 24]. Because of the difference of geological environment and lithologic composition, the research results cannot reflect the hydration damage law of continental oil shale reservoir. Secondly, high-quality continental source rocks in China often coexist with tuff, which is an important feature of shale oil reservoir [25]. Tuff is a volcanic rock which is easy to hydrate. Tuff must be considered in the study of hydration damage and permeability characteristics of shale oil reservoir, which is lack of existing research. Finally, different from the bedding structure within the same lithology, the laminar structure is formed by overlapping of different lithology. Continental shale oil contains lamellar structure, which makes it more heterogeneous than marine shale [26].

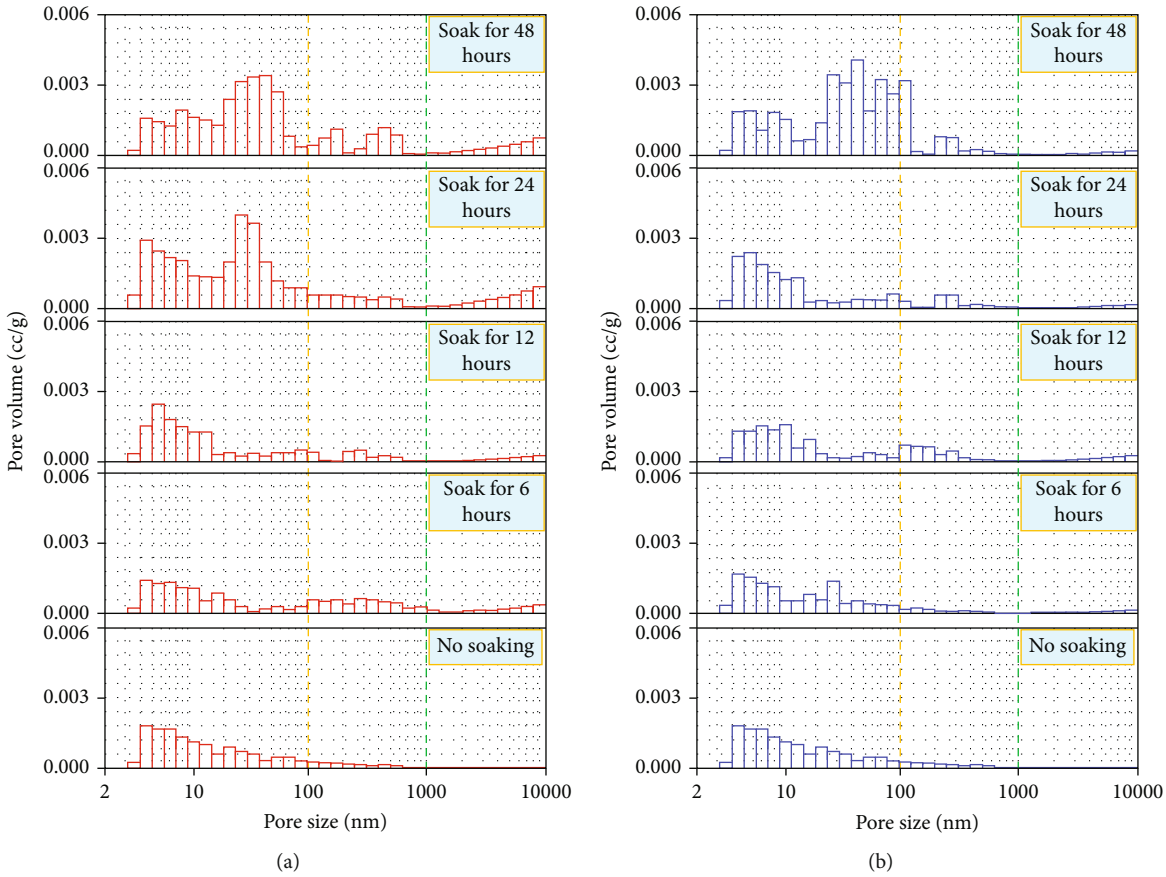

Figure 5: Influence of fluid invasion on shale's pore size distribution. (a) Relationship between pore distribution and water soaking time. (b) Relationship between pore distribution and water-based drilling fluid soaking time.

In this study, the downhole core in the Triassic Chang 7 Member of Southern Ordos Basin was taken as the experimental object, and the lamellar structure was analyzed by macroscopic core description, rock thin section identification, and scanning electron microscope. The pore size distribution and permeability of rock under different fluid invasion time were tested by high pressure mercury injection experiment and steady gas permeability experiment. Characteristics of hydration damage and its influence on permeability can be obtained by analyzing experimental results, which can provide support for drilling and completion operation and selection of water-based drilling fluid for lamellar shale oil reservoirs.

2. Samples and Methods

2.1. Basic Geochemical Properties. Ordos Basin is the second largest sedimentary basin in China, which is rich in mineral resources. After investigation, it is found that high-quality source rocks are developed in the Triassic Chang 7 Member, and the total organic carbon (TOC) content of the reservoir reaches 17.41% [27]. Some organizations have studied the source rock development, lithology characteristics, and pore distribution of shale oil reservoir in Chang 7 member. It is proved that the shale oil in Chang 7 member of Ordos Basin has great potential for exploitation, and several shale oil test areas have been established in the basin [28–31]. It is proved that the shale oil in Chang 7 member of Ordos Basin has great potential for exploitation, and several shale oil test areas have been established in the basin [32].

The samples in the study were taken from the BC block in the southwest of the basin (Figure 1(a)). The structure in the area is high in the southeast and low in the northwest, with developed faults. Small anticlines, fault anticlines, and nose uplifts developed locally. The core of the exploration well shows that the reservoir contains a large number of thin sandstone lamina structure, and parallel laminar fractures are developed in the shale (Figure 1(b)). The lower part contains tuff, in which bedding and structural fractures are developed (Figure 1(c)). The content of terrigenous clasts is high in the reservoir, especially in the lamellar shale section.

Zhao et al. tested the mineral composition of rocks in the work area by X-ray diffraction experiment and found that the mineral types are complex, the content of quartz and clay is high, the brittle minerals are more, and the range of mineral content fluctuation is large [34] (Figure 2).

2.2. Samples and Drilling Fluid. The rocks were collected from the depth of 1434-1447 m in the research area. On the basis of the full diameter core, the lamellar structure and

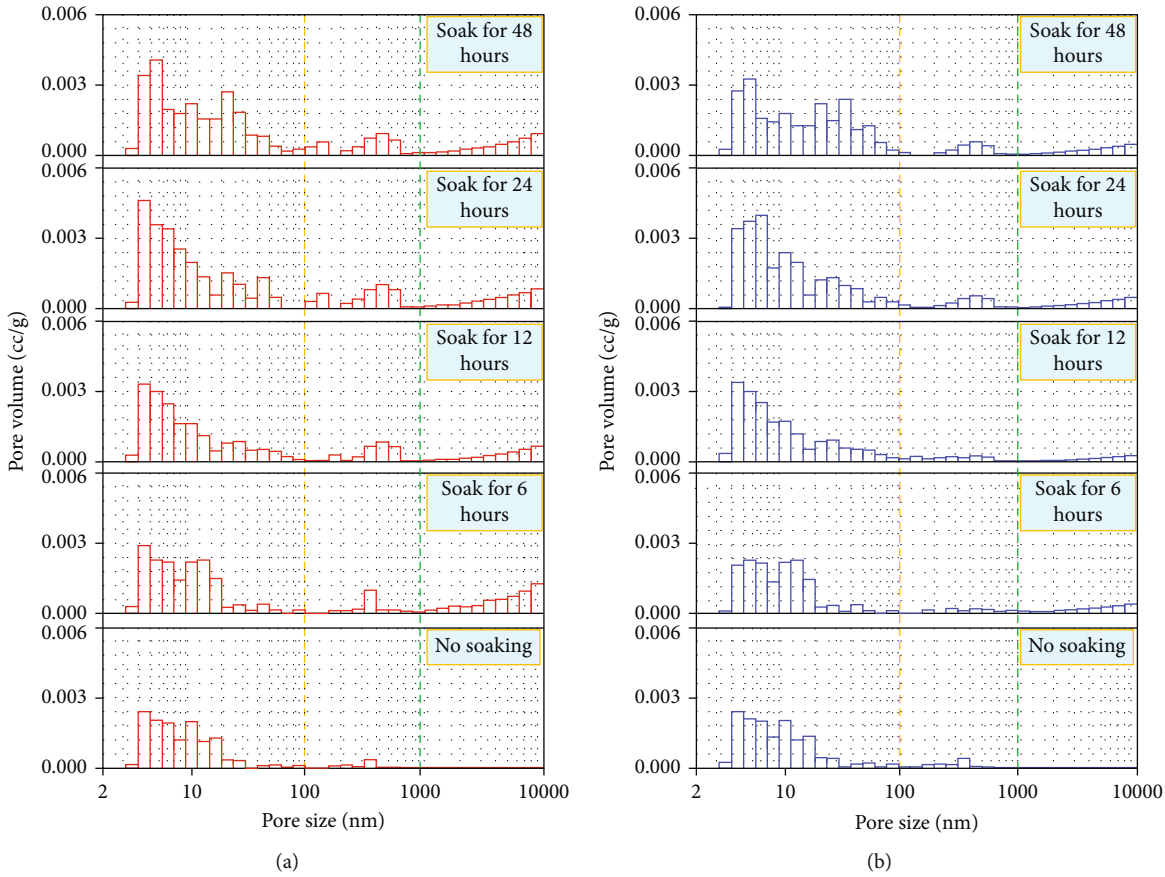

Figure 6: Influence of fluid invasion on tuff's pore size distribution. (a) Relationship between pore distribution and water soaking time. (b) Relationship between pore distribution and water-based drilling fluid soaking time.

bedding sections were taken, respectively, to prepare samples of different specifications (Figure 3). Cylinder cores with angles of 0°, 45°, and 90° from lamina were drilled for permeability test. After grinding and spraying metal, microsquare cores were used for scanning electron microscope. Rock thin sections with a thickness of 30-100 μm were used for microscope. The long strip rock debris with large specific surface area are the samples for mercury injection experiment.

The hydration damage of rock in formation was simulated by soaking the samples in water and water-based drilling fluid at 80°C. The water-based drilling fluid contained potassium sodium silicate and amino group inhibitor for inhibit hydration and was equipped with nanosized silica and asphalt for plugging. The apparent viscosity of drilling fluid is 20 mPa·s, and the apparent viscosity of drilling fluid is 20 mPa·s. The particle size of drilling fluid ranges from 0.02 μm to 200 μm, which is concentrated in 1.38 μm.

2.3. Pore Size Distribution Test. The pressure that forces nonwetting liquid to enter the pore depends on the radius of the pore, so mercury injection experiment can be used to test the pore size distribution in rock [35]. Mercury injection method is widely used in reservoir pore distribution because of its simple principle, wide testing range, and high precision [36]. The Poremaster-60 produced by Quantachrome Instruments Company was used for the mercury injection experiment. Before the experiment, the instrument was calibrated with aluminum oxide standard sample. 106 pressure points were tested for each sample, and each point was stabilized for 30 seconds.

The pore radius (R_i) can be calculated when the pressure is P_i. According to the amount of mercury injected (Q_i), the content (C_i) of pores with different radius (R_i) can be obtained. The calculation equation is given as

$$\begin{cases} R_i = \dfrac{K}{P_i}, \\ C_i = \begin{cases} Q_1 \; i = 1, \\ Q_i - \sum_{1}^{i-1} Q_n, \quad i \geq 2, \end{cases} \end{cases} \tag{1}$$

where R_i is the pore diameter at different test points, P_i is the pressure at different test points, C_i is the pore volume at different test points, Q_i is the mercury injection amount at different test points, and K is the constant of test calibration.

2.4. Permeability Test and Permeability Anisotropy Calculation. According to Darcy's law, the seepage velocity

Table 1: The influence of lithology, structure, sampling angle, fluid environment, and soaking time on permeability.

No.	Lithology	Structure	Sampling angle (°)	Soaking fluid	Permeability after soaking (mD)				
					0 h	12 h	24 h	36 h	48 h
1	Shale	Lamellar structure	0	Water	4.27	6.93	7.08	7.15	7.15
2				WBDF	3.67	4.55	5.12	5.20	5.18
3			45	Water	1.98	2.57	2.67	2.83	2.83
4				WBDF	1.56	2.01	2.12	2.22	2.19
5			90	Water	0.51	0.57	0.61	0.67	0.61
6				WBDF	0.33	0.36	0.37	0.39	0.38
7		Bedding structure	0	Water	1.48	1.51	1.64	1.70	1.71
8				WBDF	1.41	1.47	1.56	1.54	1.55
9			45	Water	1.14	1.21	1.25	1.24	1.26
10				WBDF	0.77	0.79	0.87	0.85	0.85
11			90	Water	0.36	0.39	0.39	0.39	0.40
12				WBDF	0.29	0.30	0.31	0.32	0.32
13	Tuff	Lamellar structure	0	Water	3.61	4.99	5.27	5.29	5.31
14				WBDF	3.71	4.49	4.67	4.61	4.65
15			45	Water	1.77	2.33	2.51	2.54	2.57
16				WBDF	2.24	2.91	2.87	2.89	2.97
17			90	Water	0.67	0.73	0.75	0.79	0.76
18				WBDF	0.65	0.69	0.71	0.70	0.71
19		Bedding structure	0	Water	0.89	1.09	1.20	1.23	1.24
20				WBDF	0.91	0.98	0.95	0.97	0.99
21			45	Water	0.51	0.56	0.58	0.59	0.60
22				WBDF	0.69	0.72	0.75	0.76	0.75
23			90	Water	0.45	0.49	0.51	0.52	0.53
24				WBDF	0.55	0.59	0.58	0.59	0.60

of flow through porous media is directly proportional to cross-sectional area, pressure difference, and permeability and inversely proportional to liquid viscosity and length of porous media [37]. In anisotropic lamellar shale oil reservoirs, the three-dimensional expression of Darcy formula is as follows.

$$\begin{cases} v_{\mathrm{x}} = -\dfrac{1}{\mu}\left(k_{xx}\dfrac{\partial P}{\partial x} + k_{xy}\dfrac{\partial P}{\partial y} + k_{xz}\dfrac{\partial P}{\partial z}\right), \\ v_{\mathrm{y}} = -\dfrac{1}{\mu}\left(k_{yx}\dfrac{\partial P}{\partial x} + k_{yy}\dfrac{\partial P}{\partial y} + k_{yz}\dfrac{\partial P}{\partial z}\right), \\ v_{z} = -\dfrac{1}{\mu}\left(k_{zx}\dfrac{\partial P}{\partial x} + k_{zy}\dfrac{\partial P}{\partial y} + k_{zz}\dfrac{\partial P}{\partial z}\right), \end{cases} \tag{2}$$

where v_i is seepage velocity, μ is liquid viscosity, k_{ij} is permeability tensor, and P is formation pressure. The Gasperm permeameter produced by VINCI was used in the experiment, and the temperature was 20°C, and the confining pressure was 230 psi during the experiment. Due to a large number of lamellar sandstone and obvious bedding in shale, the shale oil reservoir has significant anisotropy (Figure 4).

Yang et al. deduced that the permeability in any direction can be calculated by formula (3). By testing K_1 and K_3, the permeability at any angle with the lamellar structure could be calculated [38].

$$\begin{cases} k_{xx} = k_1\cos^2\theta + k_3\sin^2\theta = \dfrac{k_1 + k_3}{2} + \dfrac{k_1 - k_3}{v}\cos 2\theta, \\ k_{xy} = k_{yx} = (k_1 - k_3)\cos\theta\sin\theta = \dfrac{k_1 - k_3}{2}\sin 2\theta, \\ k_{yy} = k_1\sin^2\theta + k_3\cos^2\theta = \dfrac{k_1 + k_3}{2} - \dfrac{k_1 - k_3}{2}\cos 2\theta, \end{cases} \tag{3}$$

where k_1 is the permeability parallel to the laminar direction, k_3 is the permeability perpendicular to the laminar direction, and θ is the angle between the permeability direction and lamellar structure. Fluid invasion not only changes the permeability of rocks but also affects their permeability anisotropy. The permeability anisotropy of lamellar shale oil reservoir is expressed by the permeability ratio of bedding and vertical lamina, and the change rate of permeability anisotropy is calculated by formula (4).

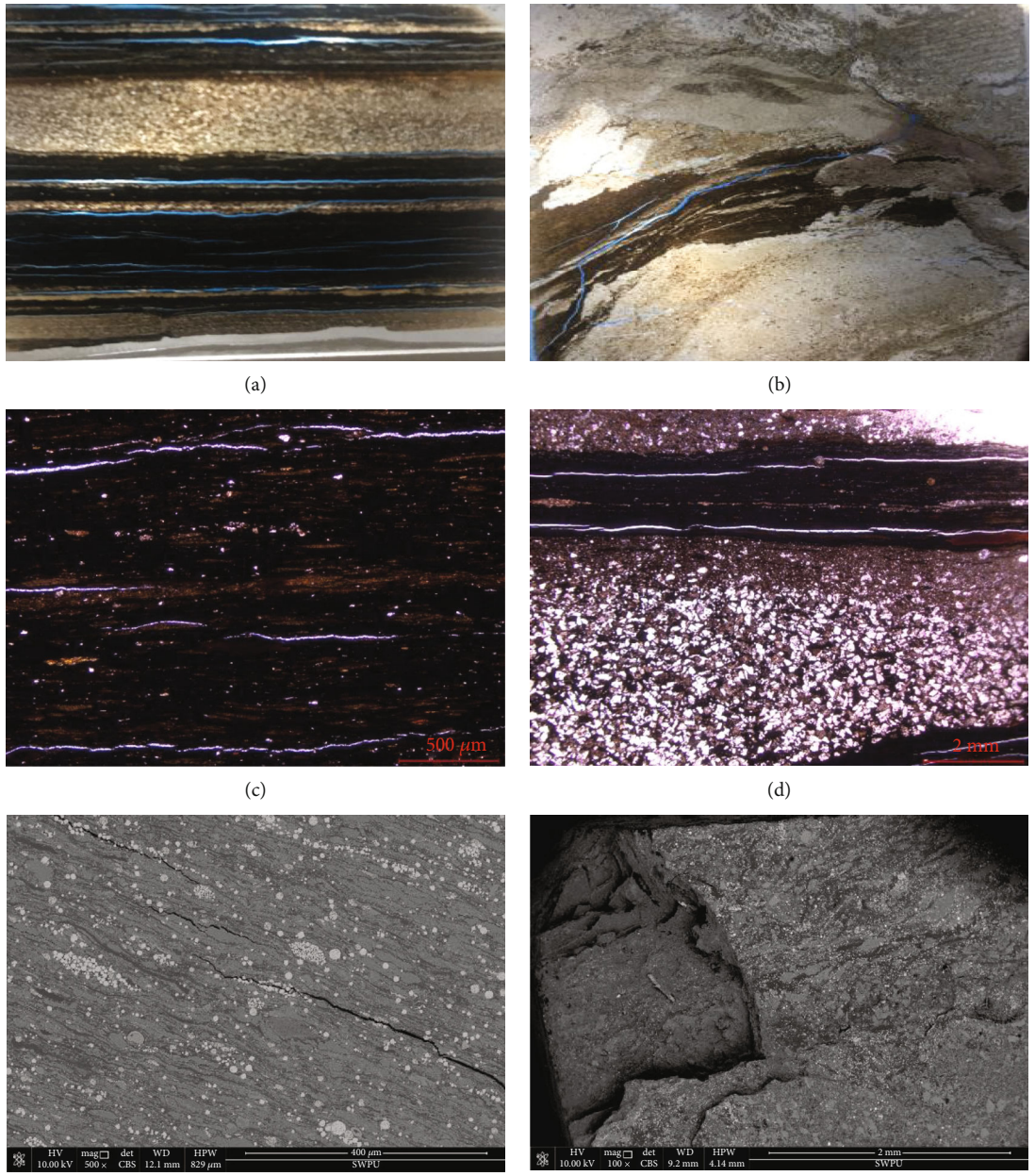

(a) (b) (c) (d) (e) (f)

Figure 7: Microstructure of laminas and beddings. (a) Fracture networks formed by superimposition of shale and sandstone laminas. (b) Deformed laminas and dendritic fractures in transition section between shale and tuff. (c) Fractures in beddings. (d) Fractures in laminas. (e) The direction of mineral arrangement and organic matter band were consistent with fractures. (f) There was obvious delamination phenomenon at the edge of the sample when the observation surface was parallel to the lamellar plane.

$$\mathrm{PA}_t = \frac{k_{t1}/k_{t3} - k_1/k_3}{k_1/k_3} \times 100\%, \tag{4}$$

where PA_t is the change rate of permeability anisotropy after different soaking time, k_{t1} is the permeability parallel to the laminar direction after different soaking time, and k_{t3} is the permeability perpendicular to the laminar direction after different soaking time.

2.5. Rock Microstructure Test. The distribution of fractures and pores can be clearly observed under the microscope through the thin section of rock injected with color glue, which is an effective method to observe the rock microstructure [39]. The rock with obvious surface features were selected to make thin sections and observed under the DM2700P microscope of Leica Instrument Co., Ltd.

Scanning electron microscope (SEM) is an important method to observe tight reservoir, which can display the

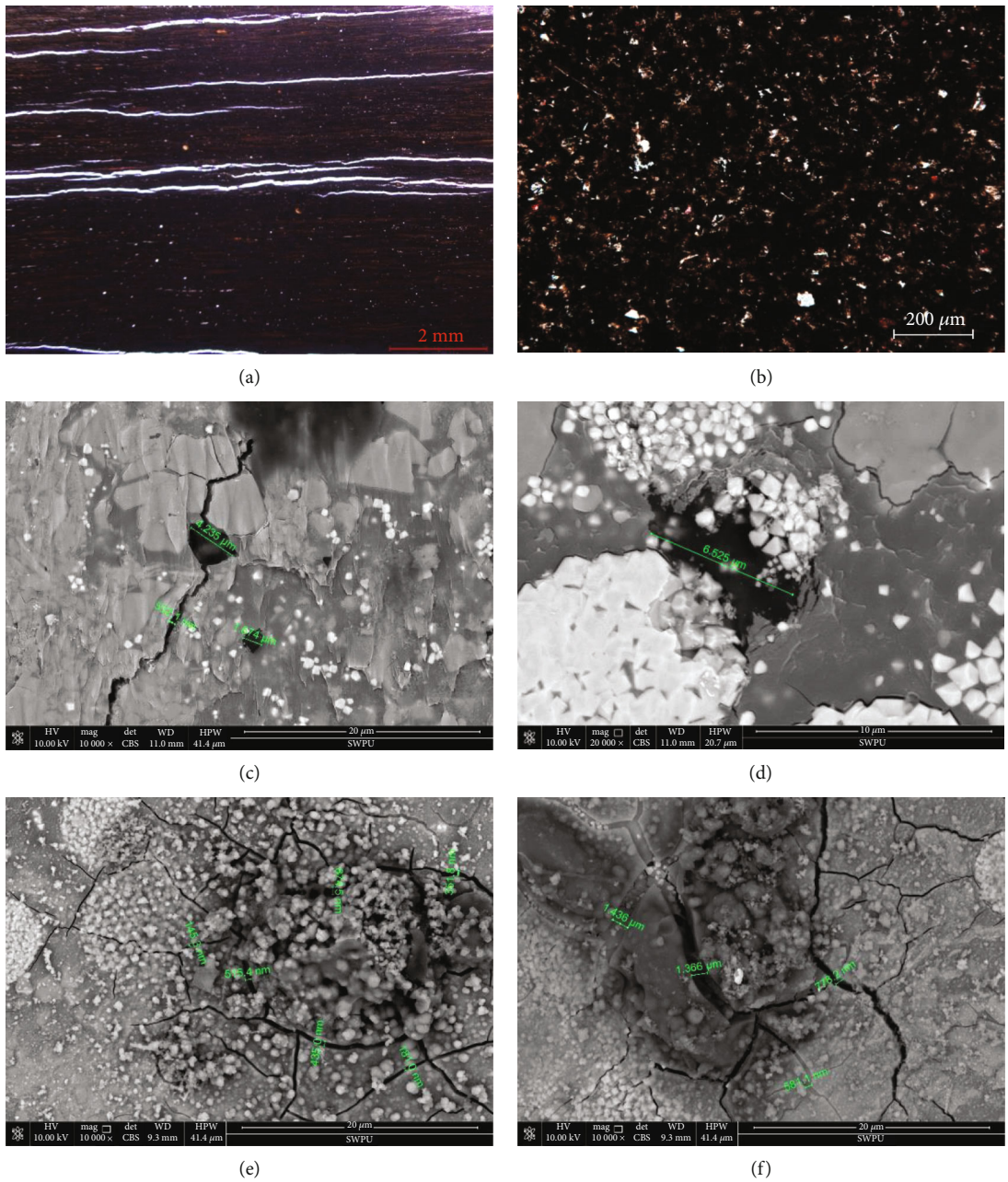

(a) (b) (c) (d) (e) (f)

Figure 8: Microstructure of laminas and beddings after soaking. (a) Rock thin section after soaking in water. (b) Rock thin section after soaking in water-based drilling fluid. (c) The mineral on the rock surface fell off after soaking in water. (d) The pyrite coated with organic matter fell off after soaking in water. (e) Bentonite and solid particles in drilling fluid formed mud cake around pyrite. (f) The mud cake cracked after drying and dehydrating.

structural characteristics of rocks at a high magnification [40]. After polishing, metal spraying, soaking, and drying, micro-square cores were observed under the FEI Quanta 650 FEG field emission scanning electron microscope.

3. Results

3.1. Pore Size Distribution. In order to facilitate the description and study, the pores above 1 μm were classified as large pores, the pores with 100-1000 nm were classified as medium pores, and the pores below 100 nm were classified as small pores. Figure 5 shows the pore size distribution of shale after soaking in water/water-based drilling fluid for 6 h, 12 h, 24 h, and 48 h. The pores of nonsoaked shale were mainly small and medium pores, and the pore volume decreased step by step with the increase of pore size. After soaking in water for 6 hours, large pores increased significantly, and the medium pores increased a little. After soaking in water for 6 to 12 hours, the pore volume of small pores increased significantly. After soaking in water for 12 to 24 hours, the pores of all sizes increased, and the increase of small pores was the most obvious. After soaking in water for 24 to 48 hours, the

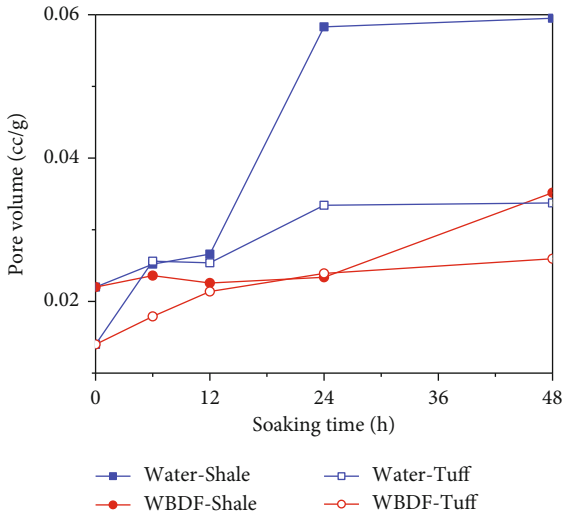

Figure 9: Variation curve of pore volume of shale and tuff with soaking time in different fluids.

total pore volume of shale was almost unchanged, and the transformation of pores with different sizes, such as the increase of 4-10 nm pores and the decrease of 10-100 nm pores, was the main feature of this stage.

The effect of water-based drilling fluid on pore size distribution is quite different from that of water-based drilling fluid. After soaking in water-based drilling fluid for 6 hours, the pores of shale were basically unchanged, which proves that drilling fluid had obvious inhibition effect on the growth of large pore at the initial stage of soaking. After soaking in water-based drilling fluid for 6 to 12 hours, large pores and the medium pores increased a little. After soaking in water-based drilling fluid for 12 to 24 hours, the small pores increased obviously, but the increase was smaller than that of the samples soaked in water. After soaking in water-based drilling fluid for 24 to 48 hours, the small pores increase greatly. The increase of total pore volume was the most obvious in this stage, while that of the sample soaked in water was basically unchanged.

Figure 6 shows the influence of fluid invasion on tuff's pore size distribution. The pore size of nonsoaked tuff was mainly concentrated in 4-12 nm. After soaking in water for 6 hours, the large pores increased significantly, and small pores around 10 nm also increased slightly. After soaking in water for 6 to 12 hours, the medium pores and small pores larger than 10 nm increased. After soaking in water for 12 to 48 hours, the pore volume of medium and large pores was basically unchanged, while that of small pores was increased. Under the influence of water, the large pores of tuff increased most obviously in the first 6 hours, the medium pores increased most obviously in 6 to 12 hours, and the small pores increased most obviously in 12 to 24 hours. The water-based drilling fluid also affected the pore size distribution of tuff caused by hydration. In the initial 6 hours of drilling fluid soaking, a small number of large pores appeared in the tuff, but the growth rate was less than that of the samples soaked in water. The tuff in water showed obvious medium pore's growth in 6-12 hours, while the tuff in water-based drilling fluid showed the same, but smaller growth after 12 hours of soaking.

By comparing the effects of water and water-based drilling fluid on the pore size distribution, it can be concluded that water-based drilling fluid can inhibit the growth of large pores and medium pores obviously in the experiment. The pore size changes of samples in water-based drilling were later than those in water, which proves that water-based drilling fluid delayed the hydration of rocks.

3.2. Permeability and Its Anisotropy. The permeability test results showed that the reservoir permeability was generally lower than 5 mD (Table 1). The k_1/k_3 of shale and tuff with laminar structure could reach 11.1 and 5.7, while the values were 4.8 and 1.9 in shale and tuff without lamellar structure, which indicated that the permeability anisotropy of shale with lamellar structure was the strongest. The permeability is vector, and the lamellar structure makes the permeability of shale oil reservoir obviously anisotropic. The permeability of samples with lamellar structure was higher than that of samples without lamellar structure, and this phenomenon was most prominent when the sampling angle is 0°.

The soaking time and the type of fluid would change the original permeability of samples. Compared with water, water-based drilling fluid reduced the increase of permeability by inhibiting the growth of pores. According to the experimental results, the permeability of samples changed obviously in the initial 24 hours after soaking and tended to be stable after soaking 48 hours. The results show that the permeability of the samples could be increased by increasing the lamina, soaking in water, increasing the soaking time, and reducing the angle between the permeability direction and the lamina or bedding, and the effects of increasing the lamina and changing the permeability direction were the most obvious.

3.3. Microstructure. The density of laminas in rock thin sections was high, and shale laminas and sandstone laminas overlapped each other to form fracture networks (Figure 7(a)). In the lithology of the transition section between shale and tuff, the content of argillaceous and tuffaceous was high, which would form deformed laminas and dendritic fractures (Figure 7(b)). Under the microscope, it can be seen that there were considerable fractures in the lamellar rock (Figure 7(c)) and bedding rock (Figure 7(d)), and the fractures in the lamellar rock were generally longer and wider than those in the bedding rock. Under the SEM, it could be seen that the direction of mineral arrangement and organic matter band in the rock were consistent with fractures (Figure 7(e)), which proved that the orderly deposition of minerals had an impact on the fracture extension direction. When the observation surface of the sample was parallel to the lamellar plane, there were few fractures on the observation surface but were obvious delamination at the edge of the sample (Figure 7(f)), which proved that the fractures were concentrated on the lamellar and bedding planes.

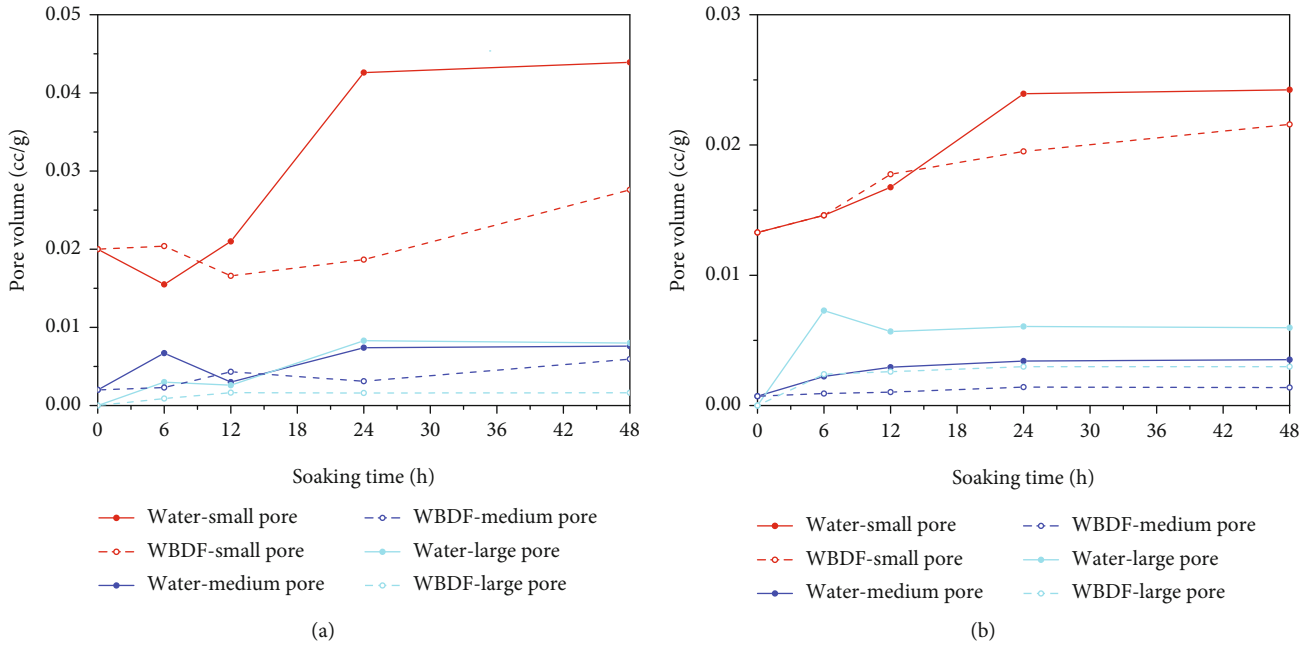

Figure 10: Variation curve of pore volume of different pore sizes with soaking time in different fluids. (a) Shale. (b) Tuff.

Figure 8 shows the microstructure of the sample after soaking in water and water-based drilling fluid for 24 hours and drying in a blower at 80°C for 12 hours. There were still a large number of fractures in the rock thin section after soaking in water (Figure 8(a)). After soaking in water-based drilling fluid, the surface of rock thin section was filled with bentonite, and no obvious fracture was found under the low magnification (Figure 8(b)). Under the SEM with a higher magnification, it was found that the mineral exfoliation occurred on the surface of the sample after soaking in water (Figure 8(c)), especially around pyrite wrapped by clay and organic matter (Figure 8(d)). After soaking in water-based drilling fluid, bentonite and plugging particles accumulated in the surface with high permeability to form plugging mud cake, and the mud cake cracked after drying and dehydrating (Figures 8(e) and 8(f)).

4. Discussion

4.1. Change of Pore Size Distribution Caused by Hydration Damage. Figure 9 is the variation curve of pore volume of shale and tuff after soaking in water and water-based drilling fluid. After soaking for 48 hours, the pore volume of shale and tuff in water increased by 170.5% and 140.9%, respectively, while that in water-based drilling fluid increased by 59.8% and 89.2%. After soaking for 6 hours, the pore growth of shale and tuff in water-based drilling fluid was smaller than those in water, while the pore growth of shale and tuff in the two fluids was close after soaking for 12 hours. After soaking for 24 hours, the pore volume of shale in water-based drilling fluid was much smaller than that in water, while this phenomenon occurred in tuff after soaking for 48 hours. The experimental results show that shale has stronger hydration reaction than tuff at the initial stage of immersion, while the effect of hydration on tuff is longer.

Further study on the change of pore size in the hydration process showed that the change of the small pore was the most obvious, especially in shale (Figure 10). The growth rates of the small and medium pore of shale in water were 119.5% and 28.1% after 48 hours soaking, while those in water-based drilling fluid were 38.1% and 19.6%. At the same time, the increase of the large pore in water-based drilling fluid was 79.6% less than that in water, which showed that water-based drilling fluid had obvious inhibition effect on small and large pores in shale (Figure 10(a)). The growth rates of the small and medium pore of tuff in water were 82.4% and 391.2% after 48 hours soaking, while those in water-based drilling fluid were 62.4% and 92.9%. At the same time, the increase of the large pore in water-based drilling fluid was 50.2% less than that in water, which showed that water-based drilling fluid had obvious inhibition effect on medium and large pores in tuff (Figure 10(b)). According to the observation results of microstructure, large pores mainly formed by mineral shedding and fracture extension, which proved that water-based drilling fluid had obvious effect on strengthening mineral particles on rock surface and preventing fracture extension.

4.2. Effect of Hydration on Permeability Anisotropy of Lamellar Shale Oil Reservoir. The change of permeability with soaking time under different lithology, rock structure, fluid environment, and sampling angle is shown in Figure 11. The permeability of lamellar samples gradually tended to be stable after soaking for 12 hours, which was earlier than that of bedding samples. This phenomenon proved that hydration had a rapid effect on the permeability of lamellar samples. During the soaking process, the increase

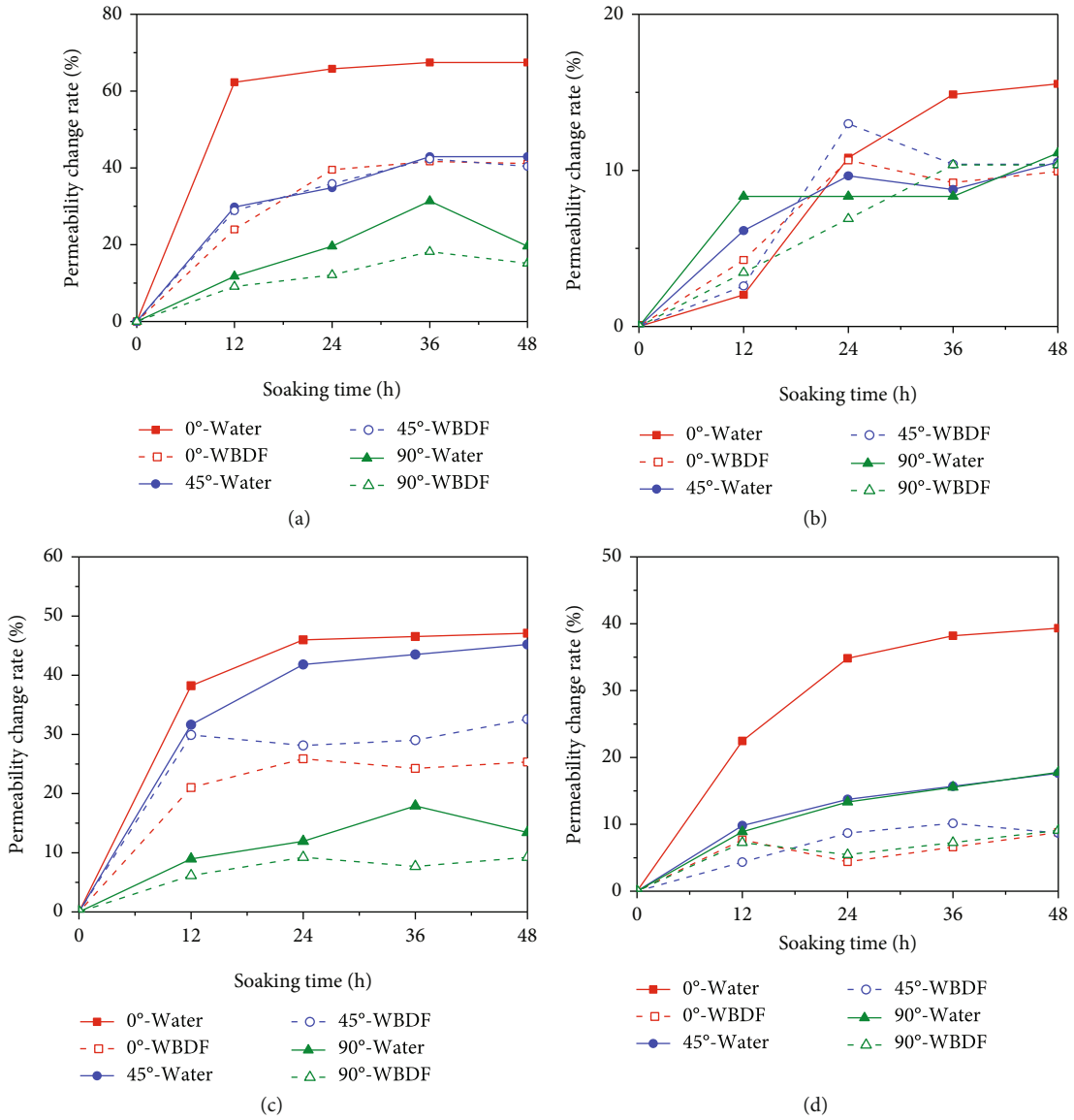

Figure 11: Variation curve of permeability with soaking time under different lithology, rock structure, fluid environment, and sampling angle. (a) Lamellar shale. (b) Bedding shale. (c) Lamellar tuff. (d) Bedding tuff.

of permeability in water-based drilling fluid was smaller than that water, and the difference was most obvious when the permeability direction was parallel to the lamina or bedding. The permeability of lamellar samples increased more than that of bedding samples, especially in shale, which proved that lamellar structure aggravated the influence of fluids on rock permeability.

The permeability was positively correlated with the soaking time in general, because the pore volume increased with the increase of soaking time, which was consistent with the results of the mercury injection experiment. The permeability of some samples decreased slightly with the increase of soaking time in some stages, which might lead by repeated shedding and adhesion of clay, mineral debris, and plugging particles in the permeability channel due to the continuous soaking and drying process.

According to formula (4), the influence of lithology, rock structure, and fluid environment was calculated as shown in Figure 12. The results show that the permeability change rate of lamellar samples was larger than that of samples without lamellar structure, whether immersed in water or water-based drilling fluid. Under the same lithology, rock structure, and soaking time, the permeability anisotropy of samples in water-based drilling fluid was smaller than that in water, which proved that the hydration could increase the permeability anisotropy of shale oil reservoir rock, and the influence can be reduced by adding inhibitor and plugging materials in the drilling fluid. Compared with rock structure and fluid environment, the influence of lithology on permeability anisotropy was not obvious.

Lu et al. studied the effect of hydration on the bedding shale by SEM. They found that after soaking in distilled

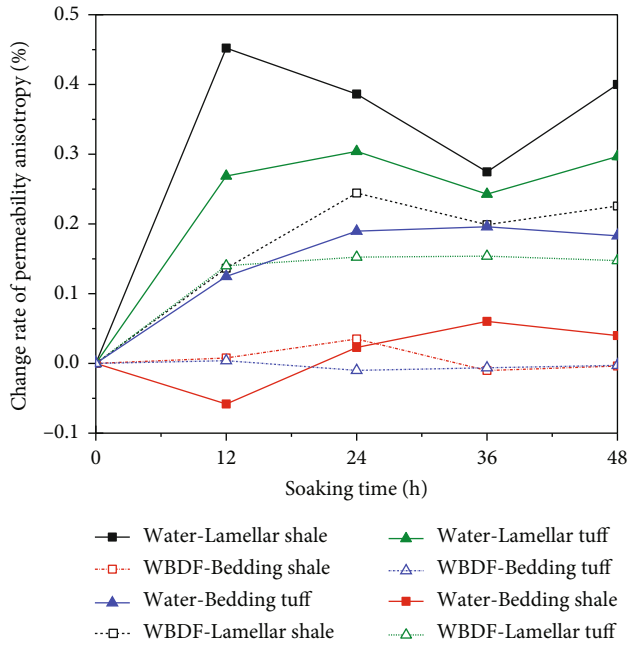

Figure 12: Variation curve of permeability anisotropy with soaking time under different lithology, rock structure, and fluid environment.

water, the width of microcracks parallel to bedding would increase, but there was no significant change in vertical bedding direction [41]. Through the experimental study, it is concluded that lamellar shale has similar properties and is more obvious than bedding shale.

4.3. Effect of Hydration on Rock Microstructure. The change of physical parameters of rock is the macroscopic manifestation of microstructure change. The results of rock thin section and scanning electron microscope showed that there were a lot of fractures near the lamellar structure, which were caused by the weak cementation between different lithology [42]. The fractures in the lamellar rock were longer and wider than those in bedding rocks. The larger fractures increased the contact area between fluid and rock and accelerated the hydration process, resulting in the permeability of lamellar rock tended to be stable earlier than that of bedding rock. The content of continental clastic rock is high in continental lamellar shale oil reservoirs. After soaking, minerals on the surface of the rock fell off and formed pores, which is the reason for the increase of large pores in the initial stage of soaking.

There are a lot of berry pyrite wrapped by clay in the lamellar shale oil reservoir of Ordos Basin. Hydration resulted in clay swelling and pyrite shedding, which increased the permeability channel of fluid. The solid particles and soil powder in the water-based drilling fluid were easy to be accumulated in the pores and fractures to form protective mud cake, which could reduce the mineral shedding and seal the pores and fractures.

5. Conclusion

To study characteristics of hydration and its influence on permeability of lamellar shale oil reservoirs, the influence of water and water-based drilling fluid on pore size distribution, permeability, and microstructure of rock was tested by taking the core of lamellar shale oil reservoir in Ordos Basin. Several conclusions are drawn as follows:

(1) The pores are mainly in nanoscale, which are concentrated below 100 nm. After soaking in water for 48 hours, the pore volume of shale increases by 170.5%, which is most obvious in 12-24 hours, and the pore volume of tuff increases by 140.9%, which is most obvious in 24-48 hours. Water-based drilling fluid can inhibit the growth of pores and delay the hydration of rocks

(2) The permeability of lamellar rocks is generally higher than that of bedding rocks. Hydration can increase the permeability of rocks, which is most obvious when the permeability direction is parallel to the laminar/bedding direction. Hydration not only increases permeability but also enhances permeability anisotropy of rocks, especially lamellar rocks

(3) Hydration leads to the formation of new pores, new fractures, and the expansion of existing fractures in rocks, especially in the strata containing large amounts of terrigenous clastic, lamellar structure, and pyrite. The new seepage channel increases the permeability of rock, and the soil powder and plugging particles in drilling fluid are easy to form protective mud cake in these places

(4) Compared with bedding rock, lamellar rock has stronger anisotropy and more fracture, and its permeability is easier affected by hydration. It is helpful for the efficient and safe development of continental shale oil to find out the occurrence and characteristics of lamina and put forward corresponding drilling and development plans

Data Availability

All laboratory data used to support the findings of this study are included within the article.

Conflicts of Interest

The authors declare that they have no conflicts of interest.

Acknowledgments

This work was funded by the National Science and Technology Program during the 13 Five-year Plan Period (Grant no. 2017ZX05049) and the National Natural Science Foundation of China (Grant nos. 51774246 and 51474185).

References

[1] C. Zou, G. Zhang, Z. Yang et al., "Geological concepts, characteristics, resource potential and key techniques of unconventional hydrocarbon: on unconventional petroleum geology,"

Petroleum Exploration and Development, vol. 40, pp. 385–399 +454, 2013.

[2] S. Hu, W. Zhao, L. Hou et al., "Development potential and technical strategy of continental shale oil in China," *Petroleum Exploration and Development*, vol. 47, no. 4, pp. 877–887, 2020.

[3] *U.S. Energy Information Administration, How Much Shale (Tight) Oil is Produced in the United States?*, 2020, https://www.eia.gov/tools/faqs/faq.php?id=847&t=6.

[4] Q. Zhou, Z. Jin, G. Yang, N. Dong, and Z. Shang, "Shale oil exploration and production in the U. S.: status and outlook," *Oil and Gas Geology*, vol. 40, pp. 469–477, 2019.

[5] D. Li, R. Li, Z. Zhu et al., "Rare earth elements geochemistry characteristics and their geological implications of lacustrine oil shale from Chang 7 oil layer in southern Ordos Basin, China," *Geological Journal*, vol. 52, pp. 119–131, 2017.

[6] X. Nie, J. Lu, R. R. Djaroun, P. Wang, J. Li, and C. Zhang, "Oil content prediction of lacustrine organic-rich shale from wireline logs: a case study of intersalt reservoirs in the Qianjiang Sag, Jianghan Basin, China," *Interpretation*, vol. 8, no. 3, pp. -SL79–SL88, 2020.

[7] Q. Hu, Y. Zhang, X. Meng, Z. Li, Z. Xie, and M. Li, "Characterization of micro-nano pore networks in shale oil reservoirs of Paleogene Shahejie Formation in Dongying Sag of Bohai Bay Basin, East China," *Petroleum Exploration and Development*, vol. 44, no. 5, pp. 720–730, 2017.

[8] B. Liu, J. Shi, X. Fu et al., "Petrological characteristics and shale oil enrichment of lacustrine fine- grained sedimentary system: a case study of organic-rich shale in first member of Cretaceous Qingshankou Formation in Gulong Sag, Songliao Basin, NE China," *Petroleum Exploration and Development*, vol. 45, no. 5, pp. 884–894, 2018.

[9] S. Zhang, C. Liu, L. Hao et al., "Paleoenvironmental conditions, organic matter accumulation, and unconventional hydrocarbon potential for the Permian Lucaogou Formation organic-rich rocks in Santanghu Basin, NW China," *International Journal of Coal Geology*, vol. 185, pp. 44–60, 2018.

[10] Z. Jin, Z. Bai, B. Gao, and M. Li, "Has China ushered in the shale oil and gas revolution?," *Oil and Gas Geology*, vol. 40, pp. 558–570, 2019.

[11] H. Zhong, Z. Qiu, W. Huang, and J. Cao, "Poly (oxypropylene)-amidoamine modified bentonite as potential shale inhibitor in water-based drilling fluids," *Applied Clay Science*, vol. 67-68, pp. 36–43, 2012.

[12] H. She, Z. Hu, Z. Qu, Y. Zhang, and H. Guo, "Determination of the hydration damage instability period in a shale borehole wall and its application to a Fuling shale gas reservoir in China," *Geofluids*, vol. 2019, Article ID 3016563, 17 pages, 2019.

[13] P. Zhao, X. Fan, Q. Zhang et al., "The effect of hydration on pores of shale oil reservoirs in the third submember of the Triassic Chang 7 member in Southern Ordos Basin," *Energies*, vol. 12, no. 20, article 3932, 2019.

[14] X. Li, X. Yan, and Y. Kang, "Investigation of drill-in fluids damage and its impact on wellbore stability in Longmaxi shale reservoir," *Journal of Petroleum Science and Engineering*, vol. 159, pp. 702–709, 2017.

[15] X. Liu, J. Xiong, L. Liang, C. Luo, and A. Zhang, "Analysis of the wettability of Longmaxi Formation shale in the south region of Sichuan Basin and its influence," *Natural Gas Geoscience*, vol. 25, pp. 1644–1652, 2014.

[16] B. Shi, B. Xia, Y. Lin, and J. Xu, "CT imaging and mechanism analysis of crack development by hydration in hard-brittle shale formations," *Acta Petrolei Sinica*, vol. 33, pp. 137–142, 2012.

[17] T. Ma and P. Chen, "Study of meso-damage characteristics of shale hydration based on CT scanning technology," *Petroleum Exploration and Development*, vol. 41, no. 2, pp. 249–256, 2014.

[18] P. Wang, Z. Qu, and E.-M. Charalampidou, "Shale hydration damage captured by nuclear magnetic resonance," *Journal of Dispersion Science and Technology*, vol. 40, no. 8, pp. 1129–1135, 2019.

[19] W. Zhao, S. Hu, L. Hou et al., "Types and resource potential of continental shale oil in China and its boundary with tight oil," *Petroleum Exploration and Development*, vol. 47, no. 1, pp. 1–11, 2020.

[20] N. R. Backeberg, F. Iacoviello, M. Rittner et al., "Quantifying the anisotropy and tortuosity of permeable pathways in clay-rich mudstones using models based on X-ray tomography," *Scientific Reports*, vol. 7, no. 1, article 14838, 2017.

[21] Y. Ma, Z. Pan, N. Zhong et al., "Experimental study of anisotropic gas permeability and its relationship with fracture structure of Longmaxi Shales, Sichuan Basin, China," *Fuel*, vol. 180, pp. 106–115, 2016.

[22] G. Wang, D. Yang, and Z. Kang, "Experimental study on anisotropic permeability of oil shale under high temperature and triaxial stress," *Chinese Journal of Rock Mechanics and Engineering*, vol. 39, pp. 1129–1141, 2020.

[23] J. Gui, T. Ma, P. Chen, H. Yuan, and Z. Guo, "Anisotropic damage to hard brittle shale with stress and hydration coupling," *Energies*, vol. 11, p. 196, 2018.

[24] Q. Zhang, X. Fan, P. Chen, T. Ma, and F. Zeng, "Geomechanical behaviors of shale after water absorption considering the combined effect of anisotropy and hydration," *Engineering Geology*, vol. 269, article 105547, 2020.

[25] C. Zou, Z. Ynag, J. Cui et al., "Formation mechanism, geological characteristics and development strategy of nonmarine shale oil in China," *Petroleum Exploration and Development*, vol. 40, no. 1, pp. 15–27, 2013.

[26] K. Xi, K. Li, Y. Cao et al., "Laminae combination and shale oil enrichment patterns of Chang 7_3 sub-member organic-rich shales in the Triassic Yanchang Formation, Ordos Basin, NW China," *Petroleum Exploration and Development*, vol. 47, no. 6, pp. 1342–1353, 2020.

[27] Z. Li, G. Tao, M. Li et al., "Discussion on prospecting potential of shale oil in the 3rd sub-member of the Triassic Chang 7 member in Binchang block, southwestern Ordos Basin," *Oil and Gas Geology*, vol. 40, pp. 558–570, 2019.

[28] G. Chen, W. Gang, Y. Liu et al., "High-resolution sediment accumulation rate determined by cyclostratigraphy and its impact on the organic matter abundance of the hydrocarbon source rock in the Yanchang Formation, Ordos Basin, China," *Marine and Petroleum Geology*, vol. 103, pp. 1–11, 2019.

[29] H. Cao, X. Shan, P. Sun, H. Chi, and S. Du, "Geochemical characteristics of oil shale in the Triassic Chang7 subsection, southern Ordos basin, China, and palaeo-environment reconstruction," *Neues Jahrbuch für Mineralogie, Abhandlungen*, vol. 193, pp. 45–57, 2016.

[30] W. Yuan, G. Liu, L. Xu, X. Niu, and C. Li, "Petrographic and geochemical characteristics of organic-rich shale and tuff of the Upper Triassic Yanchang Formation, Ordos Basin, China:

implications for lacustrine fertilization by volcanic ash," *Canadian Journal of Earth Science*, vol. 56, no. 1, pp. 47–59, 2019.

[31] Z. Xu, L. Liu, B. Liu et al., "Geochemical characteristics of the Triassic Chang 7 lacustrine source rocks, Ordos Basin, China: implications for paleoenvironment, petroleum potential and tight oil occurrence," *Journal of Asian Earth Science*, vol. 178, pp. 112–138, 2019.

[32] Z. Huang, Y. Hao, S. Li et al., "Oil-bearing potential, mobility evaluation and significance of shale oil in Chang 7 shale system in the Ordos Basin: a case study of well H317," *Geology in China*, vol. 47, pp. 210–219, 2020.

[33] J. Cui, R. Zhu, Z. Luo, and S. Li, "Sedimentary and geochemical characteristics of the Triassic Chang 7 member shale in the southeastern Ordos Basin, Central China," *Petroleum Science*, vol. 16, no. 2, pp. 285–297, 2019.

[34] P. Zhao, X. Fan, Q. Zhang, M. Zhang, and B. Yao, "Effects of hydration on physical properties and rock microstructure of shale oil reservoir in the Triassic Chang 7 member of Southern Ordos Basin," *Energy Sources, Part A: Recovery, Utilization, and Environmental Effects*, pp. 1–19, 2020.

[35] F. Wang, K. Yang, J. You, and X. Lei, "Analysis of pore size distribution and fractal dimension in tight sandstone with mercury intrusion porosimetry," *Results in Physics*, vol. 13, article 102283, 2019.

[36] M. M. Labani, R. Rezaee, A. Saeedi, and A. Hinai, "Evaluation of pore size spectrum of gas shale reservoirs using low pressure nitrogen adsorption, gas expansion and mercury porosimetry: a case study from the Perth and Canning Basins, Western Australia," *Journal of Petroleum Science and Engineering*, vol. 112, pp. 7–16, 2013.

[37] G. Sheng, F. Javadpour, and Y. Su, "Dynamic porosity and apparent permeability in porous organic matter of shale gas reservoirs," *Fuel*, vol. 251, pp. 341–351, 2019.

[38] T. Yang, P. Jia, and W. Shi, "Seepage-stress coupled analysis on anisotropic characteristics of the fractured rock mass around roadway," *Tunnelling and Underground Space Technology*, vol. 43, pp. 11–19, 2014.

[39] S. Fang, J. He, F. Hou et al., "Reservoirs pore space types and evolution in M-5(5) to M-5(1) submembers of Majiagou Formation of Middle Ordovician in central gasfield area of Ordos basin," *Acta Petrologica Sinica*, vol. 25, pp. 2425–2441, 2009.

[40] X. Tang, Y. Zhu, and Y. Liu, "Investigation of shale nano-pore characteristics by scanning electron microscope and low-pressure nitrogen adsorption," *Journal of Nanoscience and Nanotechnology*, vol. 17, no. 9, pp. 6252–6261, 2017.

[41] Y. H. Lu, L. P. Zeng, Y. Jin et al., "Effect of shale anisotropy on hydration and its implications for water uptake," *Energies*, vol. 12, no. 22, article 4225, 2019.

[42] B. Liu, Y. F. Lu, Y. L. Meng et al., "Petrologic characteristics and genetic model of lacustrine lamellar fine- grained rock and its significance for shale oil exploration: A case study of Permian Lucaogou Formation in Malang sag, Santanghu Basin, NW China," *Petroleum Exploration and Development*, vol. 42, no. 5, pp. 656–666, 2015.